Renewable Energy 104 (2017) 50–59

Contents lists available at ScienceDirect

Renewable Energy

journal homepage: www.elsevier.com/locate/renene

Modelling methane production kinetics of complex poultry slaughterhouse wastes using sigmoidal growth functions

Aidan Ware, Niamh Power*

Department of Civil, Structural and Environmental Engineering, Cork Institute of Technology, Cork, Ireland

ARTICLE INFO

Article history:
Received 7 April 2016
Received in revised form
12 September 2016
Accepted 21 November 2016
Available online 24 November 2016

Keywords:
Anaerobic digestion
Slaughterhouse waste
Biochemical methane potential
Kinetic study
Gompertz
Logistic
Richards

ABSTRACT

The kinetic evaluation of the methane potential from poultry slaughterhouse waste streams was performed using modified sigmoidal bacterial growth curve equations (Richards, logistic, Gompertz) in order to investigate their suitability to describe the degradation patterns associated with complex substrates, primarily composed of fats. The methane potential and degradation patterns under mesophilic conditions were assessed using Biochemical Methane Potential (BMP) assays. A nonlinear least-square regression analysis was performed to fit the sigmoidal functions to the cumulative methane production curves with respect to time generated from the BMP assays. In the cases modelled the Gompertz and logistic, three parameter models, sufficiently described the methane generation of the simple substrates (dissolved air flotation sludge) with no sign of acute inhibition due to high fat contents. When dealing with more complex degradation patterns of the substrates with a higher fat content (soft offals) and increased bioavailability of the organics, the three parameter models became insufficient in describing the experimental data due to features of the original growth functions, in particularly their fixed points of inflection. In such cases the fourth parameter afforded in the Richards model became critical allowing variability in the point of inflection allowing a much better fit to the experimental curves.

1. Introduction

1.1. Poultry slaughtering industry

The slaughtering industry is a major facet of the agri-food sector, one of Ireland's largest and most important indigenous industries as measured by wealth generation (7.7% of gross value added), exports (11.5% of total merchandise exports) and employment (9.2% of total employment) [1,2]. Poultry slaughtering accounts for 3% of annual agri-food exports with a total of 76.17 million birds slaughtered in 2014 [2]. The poultry industry produced a total of 125,000 tonnes of carcass weight equivalent in 2014 representing approximately 63–73% of the live weight of the slaughtered animals [3,4]. This results in high amounts, as much as 27–37% of the live weight of the animal, of organic by-products which are considered to be waste generated from this industry [4]. As regards the main solid organic wastes, there are feathers from the de-feathering process, intestinal residue or soft offal (SO) from the evisceration process as well as heads, feet and meat trimmings [5,6]. Moreover, dissolved air flotation sludge (DAF) from the wastewater treatment plant of the slaughterhouse is generated. These organic wastes are characterised by high organic content mainly composed of animal proteins and fats [7–9]. They are strictly managed by legislation, Animal By-Products Regulation (ABPR) 1069/2009/EC, in order to prevent the outbreak and spread of diseases [10].

Anaerobic (AD) is a robust technology and its application for the treatment of organic wastes has been emerging in recent years with an annual growth rate of 25% [11]. The use of AD as a treatment method has multiple benefits including its application on both small and large scale, generation of a multifaceted gaseous fuel that can be employed as a renewable energy resource etc.. *Appels* et al. lists and discusses the main beneficial properties of AD as well as current trends in research [11]. AD, is an approved treatment method for animal by-products according to the ABPR, is a promising alternative for the treatment of these solid organic wastes [10,12]. In AD the organic waste is converted to biogas, primarily methane, and a nutrient rich digestate through a series of biochemical processes. The methane produced can be utilised for energy production while the nutrient rich digestate can be used for

* Corresponding author.
E-mail address: niamh.power@cit.ie (N. Power).

http://dx.doi.org/10.1016/j.renene.2016.11.045

example as a soil conditioner [7]. This alternative treatment method is an effective option, combining material recovery as well as energy production allowing the possibility of moving towards an energy self-sufficient industry as well as incorporating a holistic waste treatment method [6–8,13].

1.2. Biochemical methane potential assays

As the AD of organic industrial wastes is becoming more established as a sustainable approach for waste management and energy recovery, the demand and necessity to find suitable substrates is continuously increasing. The BMP test is increasingly being recognised as a viable method to explore and determine the feasibility of a material to serve as a substrate in AD [14]. BMP assays provide an array of information on the substrate including how fast and how much of the material can be degraded under optimal conditions, as well as the potential methane yield from the material. A primary output of BMP assays is cumulative methane production curves, where the cumulative specific methane production is plotted against time. The patterns these curves follow are far from trivial and have meaningful implications on the degradation of the substrate. The kinetics of the different stages of the AD process (hydrolysis, acidogenesis, acetogenesis and methanogenesis) and ultimately the shape of the methane production curves is primarily controlled by the biodegradability characteristics of the substrate, the production of inhibitory intermediate fermenters and the performance of the methanogenic bacterial populations [15]. Some typical cumulative methane production curves are shown in Fig. 1. Labatut et al. (2011) outlines their relevance in aiding and identifying important biodegradability characteristics of the substrate and any inhibition issues [15]. The evaluation of these curves can be significantly aided using mathematic modelling of the kinetics of the methane production, allowing further insight into the behaviour of the substrate during the AD process.

1.3. Evaluation of cumulative methane curves using kinetic modelling

Modelling of microbial growth has been used to estimate various parameters, such as the specific growth rate and lag time (1) to study microbial growth rate under different conditions, (2) to evaluate the effects of antimicrobials under investigation, (3) to formulate appropriate microbiological media, or (4) to construct prediction models for use in food and fermentation microbiology [17]. Growth curves are a tool used in all such studies to describe how a variable increases over a particular time interval, until it approaches its saturation value. Bacterial growth curves typically demonstrate a phase in which the specific growth rate begins at a value of zero (minimum asymptote) and then accelerates to a maximum growth rate (μ_m) in a certain period of time denoted as the lag phase (λ), see Fig. 2. In addition the growth curves contain a final phase in which the growth rate decreases and finally reaches zero, so that a point of saturation or the maximum asymptote (A) is reached. Indefinite growth does not take place other than in the initial moments, since in nature it is not logically or physically viable. Consequently, a curve to represent a growth process will typically present as a sigmoidal curve as shown in Fig. 2, with a lag phase just after $t = 0$ followed by exponential phase and then by a stationary phase [18]. This can be related to the characteristic shape of cumulative gas production curves seen from BMP assays where three similar phases are observed 1) the phase of slow gas production (lag phase), 2) the phase of rapid gas production (exponential phase), 3) the phase in which the rate of gas production slows and eventually reaches zero (asymptotic or stationary phase).

During the lag phase the initial breakdown of insoluble substrates occurs through the hydrolytic bacteria. When the substrate is physically broken down and becomes available to the acidogenic, acetogenic and subsequently the methanogenic bacteria the phase of exponential gas production is reached. During this phase the most easily degradable portions of the substrate are degraded first, leavening an increasingly less digestible portion of the substrate. Finally the remaining non degradable portion of the substrate is left and the gas production reaches zero. The commonality between bacterial growth curves and the cumulative gas production curve in BMPs suggest that biogas production should obey sigmoidal functions [17,19]. Fitting sigmoidal functions to the cumulative methane production curves obtained from BMPs allows further information to be gathered on the performance of the substrates under anaerobic conditions; such as if the maximum methane yield was reached (A), the maximum rate of methane production (μ_m) as well as the duration of the lag phase (λ).

1.3.1. Existing sigmoidal models

A number of sigmoidal models are found in literature, such as the models of Gompertz, Richards, Stannard and logistic model [17,18]. Most of the equations describing sigmoidal growth curves contain mathematical parameters (a, b, c…) rather than parameters with biological meaning (A, μ_m and λ). This makes it difficult to estimate start values if they have no biological meaning. Zwietering et al. modified some of these equations in such a way that they

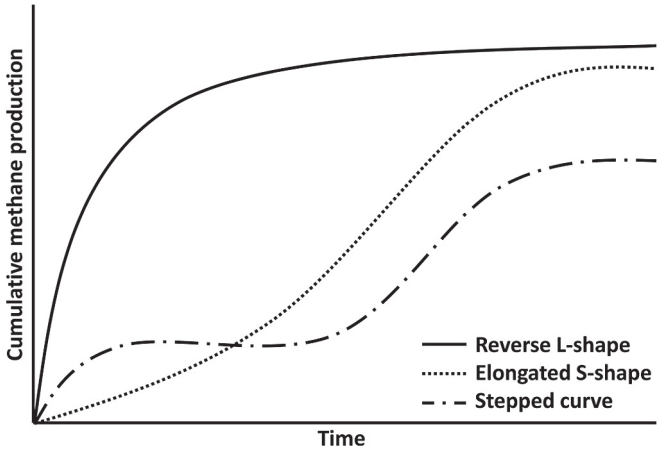

Fig. 1. Examples of typical cumulative methane production curves [15,16].

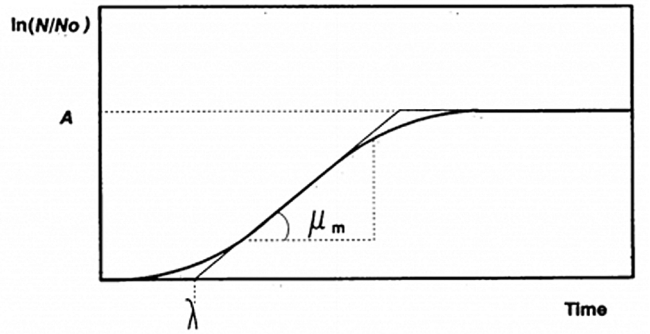

Fig. 2. Typical bacterial growth curve [18].

contain parameters that are microbiologically relevant as shown in Table 1 [18].

Once modified the Richards and the Stannard equation become the same. The Richards model, which is a generalisation of the logistic model, introduces a fourth parameter v, which allows some flexibility in the shape of the curve. For $v = 0$ and 1 the Richards model is reduced to the Gompertz and logistic model respectively [17,20]. The biological parameters determined from these modified equations are achieved as follows: μ_m is given by the slope of the line during exponential gas production (tangent to point of inflection), λ is the x-axis intercept of this slope and A is the y-axis intercept of the highest point of the curve (see Fig. 2).

1.3.2. Kinetic modelling of complex substrates

The kinetic modelling of the methane production from laboratory evaluation of substrates is becoming more and more common in literature. The modified Gompertz equation, typically applied to the degradation of simple organic substrates, is the most commonly used model for the determination of methane production kinetics. These simple substrates adopt the reverse L-shape curve shown in Fig. 1. For more complex substrate that contains a high level of animal fats the degradation patterns observed are typically not as straight forward. The slower degradation of the fats as well as the potential of acute inhibition results in curves more related to the elongated S-shape or the stepped curve. The three parameter Gompertz equation becomes less suitable to such shapes due to its fixed point of inflection; as such a fourth shape parameter needs to be introduced as is done in the Richards model.

1.4. Focus of paper

This paper assess the degradation patterns of the organic waste streams produced in the poultry slaughtering process using BMP assays and kinetic modelling. The primary aim is to demonstrate the inadequacies of three parameter sigmoidal kinetic models to accurately describe the methane production kinetics of complex substrates. A number of popular modified bacterial growth curves, Richards, logistical and Gompertz models, were applied to assess their applicability to the different forms of methane production kinetics observed from the BMP assays.

2. Materials and methods

2.1. Substrates

The slaughterhouse wastes were sampled from a poultry (broiler chickens) slaughtering facility with a capacity of 150,000 heads per week, located in Cork, Ireland. The slaughtering process employed at the facility was to the point of whole and chilled carcass production with no further processing for meat cutting or deboning. SO (not including heads and feet) from the evisceration process and DAF from the wastewater treatment were sampled for this study. The SO and DAF were also mixed according to their annual production ratios (1:1.84-SO:DAF) referred to as SHWM from this point onward. This was done to investigate the implications of treating the two waste streams collectively. The SO was tested in an un-pasteurised (SO) and pasteurised (PSO) state as per the ABPR regulations for category 3 material.

2.1.1. Sampling

The primary sample was provided by the slaughtering facility grounded on providing a typical representation of the waste streams generated during a shift of slaughtering. The consistency of the primary samples did not permit their direct use in accurate BMP assays or composition analysis. As such the entire primary samples were firstly macerated in order to reduce the particle size (<8 mm) and then blended using a high rate paddle mixer until maximum "homogeneity" was achieved. This preparation process improved the homogeneity of the primary samples considerably. However it is important to note that even after the preparation process the offals are still characterised as heterogeneous, which needs to be taken into account when considering the preparation of secondary samples for reference analyses and BMP testing as well as when considering the results [7]. Three dimensional sampling of the prepared primary sample was carried out in order to ensure representative secondary sampling of the substrates.

2.2. Analytical methods

The composition analysis was carried out in terms of basic, organic and elemental characterisation. The basic parameters used for substrate and inoculum description were the Total Solids (TS) and Volatile Solids (VS) content determined in accordance to Method 1684 of the U.S. EPA for Total, Fixed and Volatile Solids in Water, Solids and Biosolids [21]. The organics (VS) within the substrates were further broken down into primary constituents of fats, proteins and carbohydrates. Fats and proteins were determined by an approved laboratory for the microbiological testing of ABP in accordance with Commission Regulation 142/2011/EU implemented by the ABPR [10,22]. The difference between VS, fats and protein content was designated as carbohydrates. The elemental composition (C, H, N) was determined following the standard operating procedure of a CE440 Elemental Analyser, with O being designated as the difference between VS and the C, H and N content.

2.3. Biochemical methane potential assays

The methane potential of the solid organic waste streams was determined using BMP assays under mesophilic conditions (39 °C).

Table 1
Models use in bacterial growth and their modified forms according to Zwietering et al. [18].

Model	Equation	Modified equation
Logistic	$y = \frac{a}{[1+\exp(b-cx)}$	$y = \frac{A}{\left\{1+exp\left[\frac{4\mu_m}{A}(\lambda-t)+2\right]\right\}}$
Gompertz	$y = a.\exp[-\exp(b-cx)]$	$y = Aexp\left\{-exp\left[\frac{\mu_m \cdot e}{A}(\lambda-t)+1\right]\right\}$
Richards	$y = a\{1+v.\exp[k(\tau-x)]\}^{(-1/v)}$	$y = A\left\{1+v.\exp(1+v).\exp\left[\frac{\mu_m}{A}\cdot(1+v)\left(1+\frac{1}{v}\right)\cdot(\lambda-t)\right]\right\}^{(-1/v)}$
Stannard	$y = a\left\{1+exp\left[-\frac{(l+kx)}{p}\right]\right\}^{-p}$	$y = A\left\{1+v.\exp(1+v).exp\left[\frac{\mu_m}{A}\cdot(1+v)\left(1+\frac{1}{v}\right)\cdot(\lambda-t)\right]\right\}^{(-1/v)}$

y: cumulative specific methane production ($mLCH_4\ gVS^{-1}$), A: maximum specific methane production potential ($mLCH_4\ gVS^{-1}$), μ_m: max. specific methane production rate ($mLCH_4\ gVS^{-1}\ d^{-1}$), e: exp(1), λ: lag-phase (days), t:incubation time (days), v: shape coefficient.

The BMP protocol followed in this study was based on principles described in DIN 38 414 (S8) and VDI 4630 with alterations to the gas measurement system for direct measurement of the methane fraction of the biogas produced [16,23–25]. A graphical representation of the experimental set-up can be seen in Fig. 3. The BMP procedure employed was described in Ware and Power 2016a [24]. The inoculum employed was sourced from a mesophilic reactor treating dairy processing waste and was pre-incubated under the same temperature range as the operational temperature of the BMPs to deplete any residual biodegradable organic material. The pre-incubated inoculum resulted in lowered volumes of background gas being produced in the BMP assays. The inoculum to substrate ratio for all of the BMP assays was 2 based on VS content. The assays were performed in a working volume of 900 mL using a 1000 mL reactor. The large reactor size employed was to ensure an adequate sample size to allow representative sampling of the organic waste streams, due to their heterogeneous nature. Triplicate BMP assays were carried out for each of the solid waste streams and were incubated for a period of 30 or 50 days in tandem with triplicate control assays, containing only inoculum in the same quantity as the active reactors in order to estimate the background gas coming from the inoculum. The guideline for the termination of the assays was when the daily gas production was equivalent to approximately 1% of the total volume produced over the period of the test. The initial incubation period selected for this study was 30 days as the majority of the biodegradation would be completed at this stage, if required an extended period of 50 days was employed [15].

The methane production was determined directly through positive liquid displacement using an alkaline solution (0.5 M NaOH), removing the carbon dioxide fraction of the biogas. The methane production was measured daily to allow the kinetics of the process to be followed and to provide direction as to the stability of the process. At the end of the incubation period, a pH measurement was taken of all BMP assays to ensure that the methane production had not ceased due to acidification or if alkaline solution had been drawn into the reactors.

2.4. Evaluation of BMP assays

2.4.1. Potential methane yield

The net methane production from the substrate was calculated by subtracting the methane production of the control reactors from that of the active reactors. The methane potential of the substrates were evaluated based on their Specific Methane Yield (V_0) defined as the net volume of methane produced during the incubation period per amount of VS initially added to the reactor, measured as $mLCH_4\ gVS^{-1}$.

2.4.2. Kinetic modelling

A nonlinear least-square regression analysis was performed using the solver tool in MS Excel 2013 to fit the nonlinear equations (Richards, logistical and Gompertz) to the average specific cumulative methane production curves with respect to time generated from the triplicate BMP assays. This method searches for values for A, μ_m, λ with the primary objective of minimising the sum of the squares of the differences between the predicted and the measured values. The predicted specific methane yields from the nonlinear regression analysis were plotted against the measured specific methane yields in order to ascertain a visual fit to begin with. At the same time the coefficient of determination or correlation coefficient (R^2) was also obtained to determine the correlation of the model to the experimental data. The R^2 value was calculated using the regression data analysis tool in MS Excel 2013. A confidence interval of 95% was chosen for the goodness of fit of the predicted

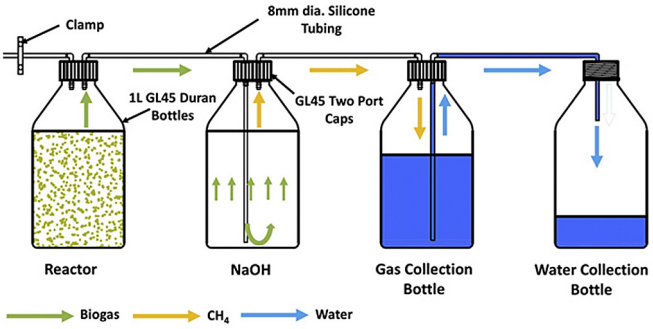

Fig. 3. Graphical representation of experimental set-up [24].

data. It is important to note that the R^2 value alone cannot be used to determine the suitability of the model; a combination of the R^2, visual inspection of the fit of the predicted and measured curves and expected parameter values must be taken into consideration, as will become evident.

It is worth noting at this time that the maximum specific daily methane yields from the BMP assays and μ_m are not specifically the same measurement. The maximum specific daily methane yields from the BMP assays are single data points giving the highest methane production in any one 24hr period. While the μ_m values are determined from the slope of the line during the exponential growth phase of the curve incorporating multiple data points, more representative to the maximum specific daily methane production to be achieved during continuous AD as oppose to batch assays.

2.4.3. Statistical analysis

All of the experiments were performed in triplicate, and the results are expressed as mean values and relative standard deviations where applicable. All statistical analysis was carried out using SPSS. Normal distribution was assumed based on the agreement of parametric and non-parametric testing and thus all inference was carried out using t-tests and a level of significance (α) of 0.05.

3. Results

3.1. Biochemical methane potential assays

3.1.1. Characterisation of organic waste streams

The characteristics of the sampled organic waste streams are presented in Table 2. The characterisation identifies the waste streams as having high organic content (93.4–96.6%) with DAF being the lowest and SO being the highest. Fat content was highest (36.1%) in the SO with SHWM and DAF showing fat contents of

Table 2
Characteristics of organic waste streams.

	DAF	SO	PSO	SHWM
TS[a]	11.7 (0.59)	40.3 (3.69)	44.9 (2.17)	24.2 (0.21)
VS[a]	93.4 (0.02)	96.6 (0.70)	96.6 (0.70)	94.8 (0.11)
Fat[b]	2.7	36.1	36.1	24.3
Protein[b]	53.5	34.0	34.0	40.9
Carb[b]	37.2	26.5	26.5	29.6
C[b]	51.6	55.3	55.3	54.0
H[b]	7.8	9.4	9.4	8.9
O[b]	25.2	26.7	26.7	25.5
N[b]	8.8	5.1	5.1	6.4

[a] % (standard deviation).
[b] % of TS.

24.3%, and 2.7% respectively. Protein was highest (53.5%) in the DAF primarily due to the high quantities of blood mixing with the wastewater, followed by SHWM, and SO at 40.9% and 34.0%. The carbohydrate content across the board is similar ranging from 26.5 to 37.2%. The high fat contents of the SO and SHWM bode well in terms of methane production with fats having a 85% and 75% higher methane potential than carbohydrates and proteins respectively [16,26]. The pasteurisation process does not alter the VS content, organic or elemental composition of the PSO as the operation temperature of 70 °C and duration of the process is too low to reduce the organic content of the samples, nor can this process add organics to the original sample [24]. That is not to say that the process did not alter the chemical structure of the organics but the overall quantity of fats, proteins and carbohydrates stayed the same.

3.1.2. Methane yield and degradation patterns

Table 3 presents the results of the BMPs including V_0, the incubation period (IP), the maximum daily specific methane yield ($V_{0d\ max}$) as well as the technical digestion period, the required time in order for 80% of V_0 to be reached. While the average cumilative methane curves of the triplicate assays for each of the substrates tested are presented in Fig. 4. The V_0 achieved ranged from 261.35 to 594.59mlCH$_4$ gVS^{-1}.

The DAF presented with the lowest V_0 at 261.35 ± 20.39 mlCH$_4$ gVS^{-1} with 80% of this being produced within the first 10 days of the IP. $V_{0d\ max}$ was observed on day 1 of the IP followed by a steady decrease in methane production over the following 7 days. The high daily methane production in the initial phase of the IP resulted in a reverse L-shape cumilative cure (see Fig. 4), typical of organic wastes containing simple organic matter that are easily hydrolysed into soluble compounds thus increasing the rate of the AD process and subsequently methane production. The lower V_0 in comparison to the other substrates was to be expected given the much lower fat content (2.7%) of the DAF and given the fact that protein and carbohydrates have a lower energy content than fats. The higher fat content of the SO and PSO (36.1%) resulted in significantly higher V_0's of 499.11 and 501.13 mlCH$_4$ gVS^{-1} respectively. However it is clear to see from the cumilative curves that the degradation patterns of these substrates differed from the simple reverse L-shape of the DAF.

The cumulative curve observed for the SO closer resembled an elongated S-shape, characterised by a high rate of methane production in the initial phase of the incubation period, followed by a decrease in daily methane yield, trailed by a significant increase in methane production at a rate that is higher than that seen in the initial phase, finally plateauing to V_0. This curve is typical for the AD of organic waste streams with high concentrations of complex compounds, in this case fats. This degradation pattern resulted in a technical digestion period of 21 days and the $V_{0d\ max}$ occurring on day 17. The elongated S-shape curve was due to the degradation rate of the fats within the SO [24]. In an anaerobic environment, fats are firstly hydrolysed to glycerol and free long chain fatty acids (LCFAs). This process is catalysed by extracellular lipases that are excreted by the hydrolytic acidogenic bacteria. The further conversion of the hydrolysis products (glycerol and LCFAs) takes place in the bacterial cells [24].

Glycerol is converted to intermediate fermenters such as acetate, volatile fatty acids (VFAs) and alcohols by the fermentative acidogenic bacteria, while LCFAs are converted to acetate (or propionate a VFA in the case of odd-number carbon LCFAs) and hydrogen through syntrophic nature of the acetogenic and methanogenic bacterial populations [8,27]. LCFAs are differentiated by their chain length, number of chemical bonds and their physical state (solid or liquid). The hydrolysis rates of fats are dependent on these chemical characteristics as well as physical characteristics such as the available surface area. The slower degradation of the fats and LCFAs resulted in a lag phase observed for the SO, indicated by the reduction in methane production for a period of time. This identified the degradation of the fats/LCFAs as the rate limiting step in the AD of the SO [24]. The gradual breakdown of the LCFAs meant that during the lag phase a steady methane production was observed. If the LCFAs were generated at a higher rate possible acute inhibition of the process may occur as seen for the PSO and SHWM.

The effect of the pasteurisation process on the methane yield as well as the biodegradation of the SO is discussed by Ware and Power 2016a [24]. In brief, the pasteurisation of the SO resulted in an insignificant increase in V_0 to 501.13 mlCH$_4$ gVS^{-1} ($p = 0.96$) [24]. However it increased the bioavailability of the organics within the substrate, in particularly the fats, indicated by the shift of the $V_{0d\ max}$ from day 17 for the SO to day 1 for the SOP ($p = 3.01 \times 10^{-5}$) [24]. The increase in bioavailability incurred the negative connotation of increased rate of formation of LCFAs to inhibitory levels causing the ceasing of methane production for a period of time. The inhibition was deemed acute and full recovery of the process occurred. This resulted in a stepped cumulative methane production curve. The combination of the PSO and the DAF waste streams to create the SHWM saw a V_o of 594.59 mlCH$_4$ gVS^{-1} a statistically insignificant increase from that of the PSO ($p = 0.08$). However, considering one tonne of the SHWM digested in its individual fractions according to the ratios of annual production the sum of the methane yield would be 416.7mlCH$_4$ gVS^{-1}. Therefore the combination of the waste streams resulted in a 42.7% increase in potential methane yield. The degradation behaviour of the SHWM was similar to that of the PSO (stepped cumulative methane curve). This was to be expected as the addition of DAF to the PSO shouldn't have a significant effect on the physical and chemical breakdown of the PSO. The high fat content and rapid degradation of LCFAs was again the cause of the acute inhibition observed in the SHWM.

3.2. Kinetic study

The modelled results using the modified Richards, logistic and Gompertz equations are plotted against the average cumulative specific methane yield measured from the triplicate BMP assays in

Table 3
Results of BMP assays.

Substrate	IP[a] (days)	V_0 (mlCH$_4$ gVS^{-1})	$V_{0d\ max}$[b] (mlCH$_4$ gVS^{-1} d^{-1})	80% of V_0 (days)
DAF	30	261.35 ± 20.39	46.19 ± 1.34 (1)	10
SO	30	499.11 ± 35.44	32.80 ± 0.39 (17)	21
PSO	50	501.13 ± 40.59	45.81 ± 0.14 (1)	36
SHWM	50	594.59 ± 38.05	45.10 ± 1.42 (23)	32

Note: relative standard deviation applied where necessary.
[a] IP- Incubation period of BMP.
[b] ( ) day on which maximum daily V_0 occurred.

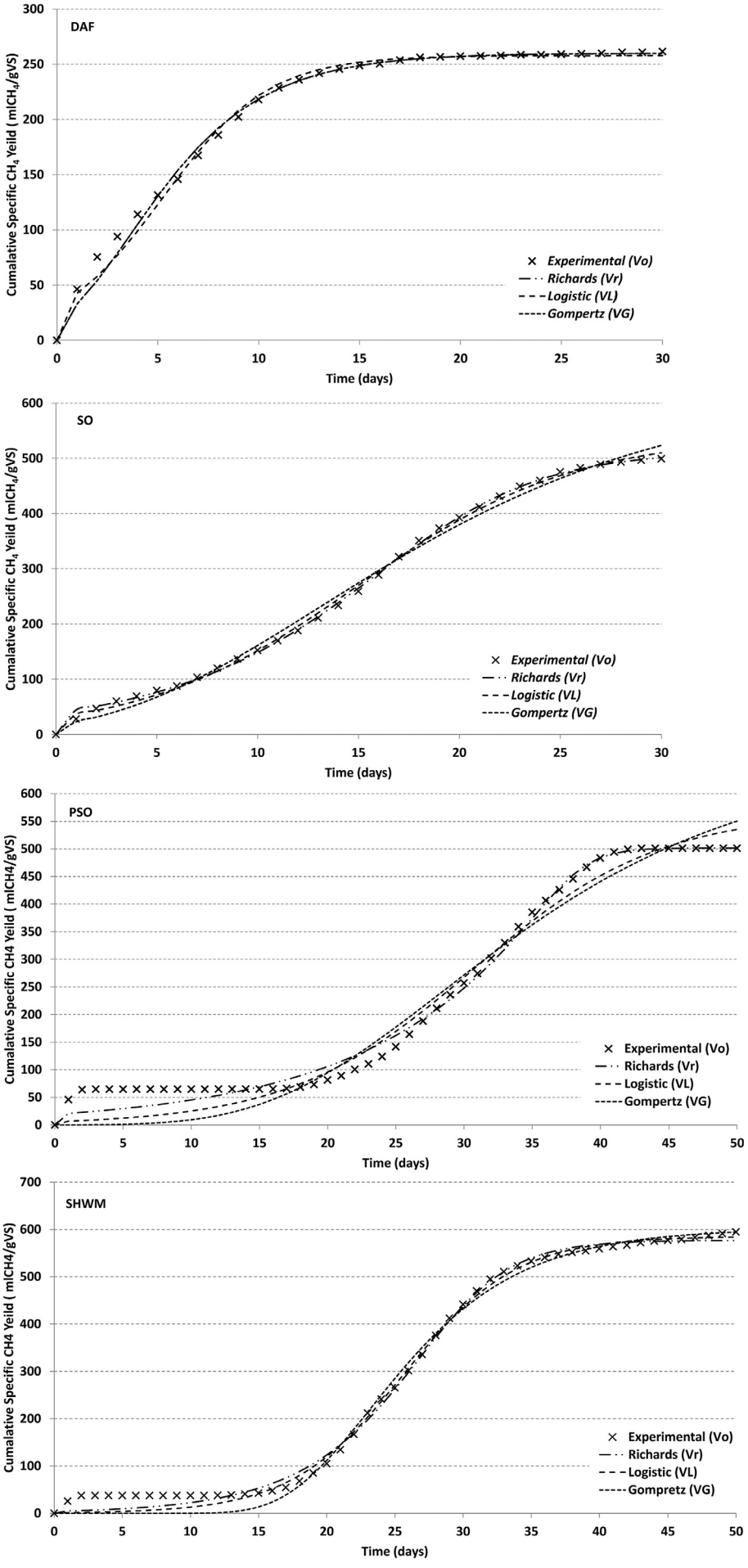

Fig. 4. Cumulative methane production fitted with models.

Table 4
Kinetic parameters of average cumulative methane production curves.

Substrate	Models	V_0 ($mLCH_4$ gVS^{-1})	A ($mLCH_4$ gVS^{-1})	μ_m ($mLCH_4$ gVS^{-1} d^{-1})	λ (days)	v	R^2	% Error V_0 and A
DAF	Richards	261.35 ± 20.39	259.98	26.31	0	0	0.995	−0.54%
	Logistic		257.83	24.62	0	_	0.995	−1.36%
	Gompertz		259.98	26.31	0	_	0.995	−0.54%
SO	Richards	499.10 ± 35.44	512.28	27.12	5.24	1.96	0.993	2.64%
	Logistic		540.51	25.36	4.35	_	0.999	8.30%
	Gompertz		634.20	22.92	3.02	_	0.996	27.07%
PSO	Richards	501.10 ± 40.59	501.67	28.61	21.93	7.78	0.991	0.11%
	Logistic		566.43	20.94	17.23	_	0.982	13.04%
	Gompertz		663.93	19.06	15.75	_	0.971	32.49%
SHWM	Richards	594.60 ± 38.05	576.87	36.88	17.92	1.86	0.997	−2.98%
	Logistic		585.25	35.42	17.35	_	0.997	−1.57%
	Gompertz		601.94	35.97	17.05	_	0.996	1.23%

Fig. 4. The parameters determined from the nonlinear regression analysis as well as the R^2 and difference between the measured V_0 and the predicted asymptotic methane production (A) are presented in Table 4.

3.2.1. DAF

From visual inspection all three models provided reasonably good fits for the experimental DAF data (see Fig. 4) while the R^2 for all three models were 0.995. All three models were observed to adequately describe methane production from the tested manures with minimal variances between the calculated parameters A, μ_m and λ observed between models. The shape factor v attained from the Richards model was 0 meaning that it reverted into the Gompertz equation as can be seen from the matching of the results from both models in Table 4.

The largest difference between the experimental specific methane yield and the modelled methane yield was 1.36%. Patil et al. reported errors of up to 8.7% when predicting methane yields from water hyacinth using sigmoidal growth curves, while Raposo et al. reported errors up to 10% in predicting methane yields from sun flower oil cake when using first-order kinetic models [28,29]. From these observations all three of the models can be reasoned as a good fit for the methane production from the DAF. This was to be expected given the relatively uncomplicated digestion of this simple substrate, i.e. no inhibition, with minimal fat content (below 3%), and proteins accounting for the majority of the organics measured resulting in characteristic cumulative methane curves compliant to the sigmoidal functions described by the models. The lag phase (λ) determined for the DAF was 0 days indicating the high bioavailability of the organic compounds within the substrates.

3.2.2. SO

Immediately it can be seen from Fig. 4 that the Gompertz and the logistic models do not provide very accurate visual fits to the experimental data of the SO, with the modelled curves seen to continue to rise at the end of the incubation period, even though the R^2 values achieved for the models fit to the experimental data was at least 0.993. If the Gompertz and the logistic models curves are extended to the asymptotic values derived in Table 4 for the SO, the inaccuracy of the visual fitness becomes much clearer (see Fig. 5).

This highlights the importance of not relying solely on the R^2 values as although the model fitted the data within the incubation period provided for the experimental results both models grossly overestimated the asymptote (A). The logistic model overestimated A by 8.30%, while the Gompertz model overestimated A by a higher degree of 27.07%. It is worth noting that this trend, Gompertz overestimating the asymptote by a higher degree than the logistic, was seen each time the models were not a suitable visual fit for the remaining substrates tested.

This resulted in the λ values being underestimated by 16.9% for logistic and 42.2% for Gompertz and μ_m being underestimated by 6.5% for logistic and 15.5% for Gompertz when compared to the Richards model. The Richards equation provided an adequate visual fit as well as high R^2 (0.993) with the calculated asymptotes varying by no more than 2.64% from the V_0 of the experimental data. The inadequate fit of the logistic and Gompertz equations can be related back to particular features of the original growth functions as presented in Table 1, as well as the biodegradation patterns observed from the BMP assays of the SO. All of the models are based on monotonically increasing functions (i.e. function always assumes that the growth rate is increasing and never equals zero or decreases) and lie between two asymptotes at $y = 0$ and $y = a$ [30]. All three functions have a single point of inflection, the point on the curve where the sign of the curvature changes from concave to convex or vice versa i.e. maximum growth rate [30,31]. The logistic and the Gompertz functions both have fixed points of inflection. The logistic function is symmetrical about its point of inflection which exists when the growth reaches half of its final growth (maximum asymptote) [30–32]. Whereas the Gompertz function is asymmetrical about its point of inflection occurring at a much earlier point than that of the logistic model, approximately $1/e$ of its final growth (maximum asymptote) [30–32]. Due to the high fat content of the SO and the various difficulties in their biodegradation, LCFA accumulation, significant hydrolytic lag phases etc. as discussed in Section 3.1, the highest rate of methane production (i.e. inflection point) of the cumulative specific methane curves is observed in the later phases of the incubation period. As such when carrying out the nonlinear least-square regression analysis both the Gompertz and the logistic functions match this latter phase of the experimental curves to the earlier sections of the modelled curves (see Fig. 5) to coordinate their relative inflection points to the maximum methane production observed in the experimental data. As the points of inflection are fixed for both these functions the remainder of the curves are modelled in accordance to the location of these points as well as the assumption of symmetry for the logistical function and asymmetry for the Gompertz. As such the maximum asymptotes are overestimated and the λ and μ_m values are underestimated as described above.

The fact that the inflection point for the logistic model occurs earlier than that of the Gompertz provides a justification as to the much larger overestimation of the Gompertz. As the curves defined by these functions are constrained by their fixed points of inflection the additional parameter of the Richards model becomes very important. The Richards equation includes an additional shape parameter (v) which allows the point of inflection of the curve to be

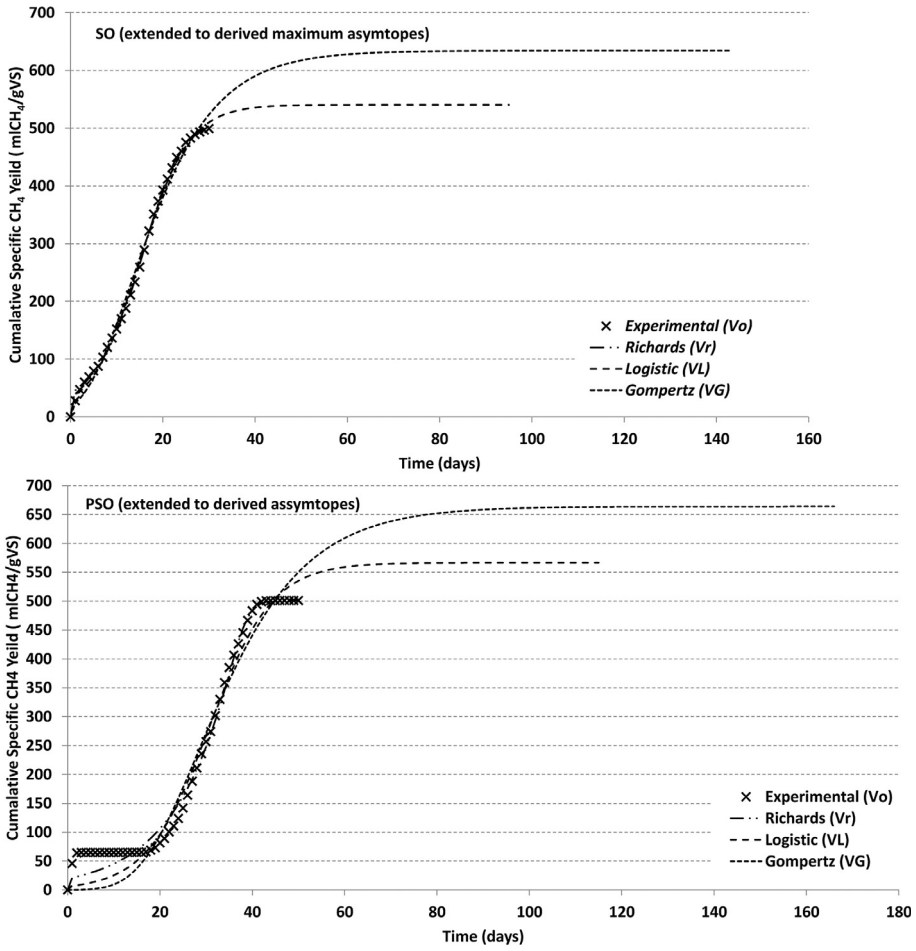

Fig. 5. Cumulative methane production fitted with models extended to predicted maximum asymptotes.

at any value between the minimum and maximum asymptote [32]. Thus allowing the model to adapt to the maximum methane production occurring at a later stage of the incubation period without any of the inherent problems observed due to a fixed inflection point as observed for the Gompertz and the logistic models. As such the Richards model provided the most accurate description of the experimental data. The high fat content of the SO resulted in a λ of 5.24 days due to the complex degradation of the fats and subsequent LCFAs. The μ_m calculated was 27.12mLCH_4 gVS^{-1} d^{-1}, occurring in the latter stages of the IP due to the delayed degradation of the fats.

3.2.3. PSO

For the same reasoning as the SO the logistic and the Gompertz models failed to accurately visually represent the experimental data for the PSO as can be seen from Fig. 5. Again the asymptotes are overestimated (greater for the Gompertz than the logistic) and λ and μ_m were underestimated. The Richards model provided a relatively good fit to the experimental data as well as R^2 values of a minimum of 0.991 and a maximum variance of 0.11% of A from the V_0 determined in the BMP assays. It is worth noting however that the visual fit of the Richards model is not faultless. This is due to the stepped curve resulting from the LCFA inhibition of the methanogenic bacteria and the subsequent temporary ceasing of methane production. The Richards model as mentioned previously is based on a monotonically increasing function, always assuming that growth/methane production is increasing between asymptotes [30]. As such the model cannot replicate the period of 0 gas production after gas production has begun. This results in the gas production during the lag phase to be underestimated initially and slightly over estimated as it reaches the very beginning of the exponential phase. However once full methanogenic recovery is reached and exponential methane production phase is reached the predicted and experimental curves are a more than adequate fit. Meaning that the determined μ_m, the slope of the line during exponential gas production (tangent to point of inflection) and λ, x-axis intercept of this slope, calculated from the Richards model can be taken as accurate representations of the biodegradation kinetics of the PSO.

As discussed in Section 3.1, pasteurisation failed to have a statistically significant effect on the specific methane yields of the offals however the process did have an effect on their bioavailability. The kinetic modelling of the P offals supported the hypothesis that the bioavailability had been increased. The increased bioavailability of the organics within the PSO resulted in rapid accumulation of LCFAs resulting in acute inhibition of the methanogenic bacteria (methane production dropped to zero and subsequently fully recovered). As a result of this an increase in λ was seen from, 5.24–21.93 days a statistically significant increases ($p = 0.007$). The increased bioavailability was most likely due to the rendering action during pasteurisation releasing the fats from the meat and tissue of the offal discussed fully in Ware and Power 2016a [24]. The μ_m achieved during the exponential phases were similar to that of the SO at 28.611mLCH_4 gVS^{-1} d^{-1}.

3.2.4. SHWM

All three models were observed to adequately describe methane production from the SHWM with minimal variances between the calculated parameters *A*, μ_m and λ determined, with the logistic and Richards models shown to have the highest correlation with a R^2 of 0.997. Again the monotonic nature of the functions can be observed in the lag phases of the SHWM curves in Fig. 4. The biodegradation patterns seen for the SHWM were similar in nature to those seen in PSO, LCFA inhibition observed in the early stages of the incubation period followed by the full recovery of the methanogenic bacteria. However the addition of the DAF to the PSO resulted in statistically significant reductions in the observed λ; 21.93–17.92 days ($p = 0.045$). This indicated that the build-up of LCFAs was not as severe with the methanogenic bacteria recovering at a quicker pace indicated by the μ_m value of 36.88mLCH_4 g$VS^{-1}d^{-1}$.

4. Discussion

The three parameter models (logistic and Gompertz) gave no difficulties in providing accurate descriptions of the experimental data and providing correct modelled parameters when dealing with substrates consisting of simple organics which degraded with no indications of inhibition or extended hydrolytic delays. Both models accurately represented the characteristic reverse L-shape curve provided by such substrates (DAF). These models, in particular the Gompertz, are the most commonly utilised kinetic model in literature [19,28,33–35]. However these three parameter models did not describe this studies data satisfactorily for complex substrates that showed rapid gas production in the latter parts of the incubation period as well as those which exhibited acute methanogenic inhibition in the early stages of the incubation period. The fixed point of inflection of both models as well as the inability to fluctuate their symmetrical (logistic) or asymmetrical (Gompertz) nature resulted in inaccurate modelled parameters being produced obvious from the poor visual fit of the predicted curves to the experimental data and overestimation of maximum asymptotes (*A*).

The fourth parameter *v* considered in the Richards equation eliminated the issues of fixed inflection points and allowed a degree of variability in the symmetry of the curves being produced. As such the Richards model provided accurate description of the complex substrates as well as those consisting of simple organics which degraded with no signs of inhibition or extended hydrolytic delays. This fourth parameter is considered a shape parameter and has no obvious biological interpretation but becomes pertinent when dealing with substrates that accumulate large quantities of intermediate fermenters such as LCFA's in the case of this study [18,32].

The kinetic parameters determined from the modelling provided further valuable insight into the results of the BMP assays in particularly the biodegradation patterns of the substrates. The low λ value seen for the DAF demonstrated their simple nature and high biodegradability. Although the BMP assays indicated that the pasteurisation process had no effect on the V_0 of the SO the kinetic modelling revealed that it did have an effect on the bioavailability of the organics, as was assumed from the BMP results. The pasteurisation process increased the bioavailability of the organics, primarily fats, which promoted more rapid accumulation of intermediate fermenters causing LCFA inhibition and increased lag phases in the PSO (5.24–21.93). The effects of mixing the slaughterhouse waste streams and digesting as a single substrate were also highlighted. The addition of the DAF to the PSO reduced the lag phases observed from 21.93 to 17.92 days and increased μ_m to 36.88mLCH_4 gVS^{-1} d^{-1}. This allowed for more rapid and stable degradation of the organics within the substrate. The parameters determined from the kinetic modelling allows for valuable insight into the biodegradation kinetics of the substrates when applied correctly. In addition to the conclusions drawn from the BMP results valuable discernment of the behaviour of each of the substrates tested can be eluded to allowing for more accurate assessments of the substrates.

5. Conclusions

In this study organic waste streams from a poultry slaughtering facility were anaerobically digested in BMP assays under mesophilic conditions. The methane yields achieved, ranging from 261.35 to 594.59mLCH_4 gVS^{-1}, are encouraging for potential energy generation from the poultry slaughtering industry. The high fat content of the SO and the SHWM resulted in almost double the methane yield observed for the DAF, with the fat content as well as pasteurisation having an effect on the process kinetics as a whole and the suitability of the various kinetic models to the experimental data. The variation in the degradation patterns caused issues when applying kinetic models to the experimental data. The three parameter Gompertz and logistic models were limited in application to the degradation patterns of more complex substrates with high fat contents. When dealing with more complex substrates the fourth parameter afforded in the Richards model allows for variability in the predicted data and thus a better fit to the experimental curves. As is the nature of biological modelling there is no one size fits all solution to the kinetic modelling of cumulative methane production from a variety of substrates. As such the conclusion of this investigation is simply stated as follows: when actual experimental data of a growth process/methane production are available, both three parameters and four models should be applied in order to determine the model of best fit.

Acknowledgments

The authors would like to thank the Irish Research Council for providing the scholarship under the Embark Initiative to allow this research to be undertaken.

References

[1] Department of Agriculture, Food and the Marine, Annual Review and Outlook for Agriculture, Food and the Marine 2013/2014. Dublin, Ireland, 2014.
[2] Department of Agriculture, Food and the Marine, Annual Review and Outlook for Agriculture, Food and the Marine 2014/2015. Dublin, Ireland, 2015.
[3] CSO (Central Statistics Office), ABA06: meat supply balance (2012-2014) by type of meat, year and statistic by type of meat, year and statistic 2013, Statbank, Available from: http://www.cso.ie/px/pxeirestat/Database/eirestat/Supply%20Balances/Supply%20Balances_statbank.asp?SP=Supply%20Balances&Planguage=0, 2013 (Accessed 10 November 2015).
[4] CSO (Central Statistics Office), Meat supply balance 2011. Cork, Ireland, Available from: http://www.cso.ie/en/statistics/agricultureandfishing/archive/releasearchive2011/, 2011 (Accessed 10 November 2015).
[5] E. Salminen, J. Rintala, Anaerobic digestion of organic solid poultry slaughterhouse waste a review, Bioresour. Technol. 83 (2002) 13–26, http://dx.doi.org/10.1016/S0960-8524(01)00199-7.
[6] Y.M. Yoon, S.H. Kin, S.Y. Oh, C.H. Kim, Potential of anaerobic digestion for material recovery and energy production in waste biomass from a poultry slaughterhouse, Waste Manag. 34 (2014) 204–209, http://dx.doi.org/10.1016/j.wasman.2013.09.020.
[7] S. Bayer, M. Rantanen, P. Kaparaju, J. Rintalal, Mesophilic and thermophilic anaerobic co-digestion of rendering plant and slaughterhouse wastes, Bioresour. Technol. 104 (2012) 28–36, http://dx.doi.org/10.1016/j.biortech.2011.09.104.
[8] J. Palatsi, M. Vinas, M. Guivernau, B. Fernandez, X. Flotats, Anaerobic digestion of slaughterhouse wastes: main process limitations and microbial community interactions, Bioresour. Technol. 102 (2011) 2219–2227, http://dx.doi.org/10.1016/j.biortech.2010.09.121.
[9] M. Edström, Â. Nordberg, L. Thyselius, Anaerobic treatment of animal byproducts from slaughterhouses at laboratory and pilot scale, Appl. Biochem. Biotechnol. 109 (2003) 127–138, http://dx.doi.org/10.1385/ABAB:109:1-3:127.
[10] EC (European Commission), 2009. Official Journal of the European Union -

European Parliament Regulation 2009/1069/EC. OJ L 300/1–14/11/2009.
[11] L. Appels, J. Lauwers, J. Degreve, L. Helsen, B. Lievens, K. Willems, J. Van Impe, R. Dewil, Anaerobic digestion in global bio-energy production: potential and research challenges, Renew. Sustain. Energy Rev. 15 (2011) 4295–4301, http://dx.doi.org/10.1016/j.rser.2011.07.121.
[12] EC (European Commission), 2005. Official Journal of the European Union - European Parliament Commission Regulation 2005/92/EC. OJ L 31/62–28/12/2005.
[13] A. Hejnfelt, I. Angelidaki, Anaerobic digestion of slaughterhouse by-products, Biomass Bioenergy 33 (2009) 1046–1054, http://dx.doi.org/10.1016/j.biombioe.2009.03.004.
[14] S. Stromberg, M. Nistor, J. Liu, Towards eliminating systematic errors caused by the experimental conditions in Biochemical Methane Potential (BMP) tests, Waste Manag. 33 (2014) 1939–1948, http://dx.doi.org/10.1016/j.wasman.2014.07.018.
[15] R.A. Labatut, L.T. Angenent, N.R. Scott, Biochemical methane potential and biodegradability of complex organic substrates, Bioresour. Technol. 102 (2011) 2255–2264, http://dx.doi.org/10.1016/j.biortech.2010.10.035.
[16] VDI 4630-Fermentation of Organic Materials: Characterisation of the Substrate, Sampling, Collection of Material Data, Fermentation Test, The Association of German Engineers, 2006.
[17] L. Altaş, Inhibitory effect of heavy metals on methane-producing anaerobic granular sludge, J. Hazard. Mater. 162 (2009) 1551–1556, http://dx.doi.org/10.1016/j.jhazmat.2008.06.048.
[18] M.H. Zwietering, I. Jongenburger, F.M. Rombouts, K.V. Riet, Modelling of the bacterial growth curve, Appl. Environ. Microbiol. 56 (1990) 1875–1881. DOI: 0099-2240/90/061875-07$02.00/0.
[19] B. Budiyono, I. Nyoman, S. Widiasa, S. Johari, The kinetic of biogas production rate from cattle manure in batch mode, Int. J. Chem. Biol. Eng. 3 (2010) 39–44. DOI: 10.1.1.309.2870.
[20] J.M. Beuvink, J. Kogut, Modelling gas production kinetics of grass silages incubated with buffered ruminal fluid, J. Anim. Sci. 71 (1993) 1041–1046. DOI: /1993.7141041x.
[21] U.S. Environmental protection Agency, Method 1684: Total, Fixed and Volatile Solids in Water, Solids and Biosolids, 2001.
[22] EC (European Commission), 2011. Official Journal of the European Union - European Parliament Commission Regulation 2011/142/EC. OJ L 59–4/3/2011.
[23] DIN 38414, Part 8: German Standard Methods for the Examination of Water, Waste Water and Sludge; Sludge and Sediments (Group S): Determination of the Amenability to Anaerobic Digestion, 1985.
[24] A. Ware, N. Power, What is the effect of mandatory pasteurisation on the biogas transformation of solid slaughterhouse wastes? Waste Manag. 48 (2016a) 503–512, http://dx.doi.org/10.1016/j.wasman.2015.10.013.
[25] A. Ware, N. Power, Biogas from cattle slaughterhouse waste: energy towards an energy self-sufficient industry in Ireland. Renewable Energy, Renew. Energy 97 (2016b) 541–549, http://dx.doi.org/10.1016/j.renene.2016.05.068.
[26] B. Drosg, R. Braun, G. Bochmann, Analysis and characterisation of biogas feedstocks, in: A.W.M. Baxter (Ed.), The Biogas Handbook, Woodhead Publishing, 2013, pp. 52–84, http://dx.doi.org/10.1533/9780857097415.1.52.
[27] D.G. Cirne, X. Paloumet, L. Björnsson, M.M. Alves, B. Mattiasson, Anaerobic digestion of lipid-rich waste-Effects of lipid concentration, Renew. Energy 32 (2007) 965–975, http://dx.doi.org/10.1016/j.renene.2006.04.003.
[28] J.H. Patil, M.A. Raj, P.L. Muralidhara, S.M. Desai, G.K. Mahadeva Raju, Kinetics of anaerobic digestion of water hyacinth using poultry litter as inoculum, Int. J. Environ. Sci. Dev. 32 (2012) 94–98, http://dx.doi.org/10.7763/IJESD.2012.V3.195.
[29] F. Raposo, R. Borja, Influence of inoculum–substrate ratio on the anaerobic digestion of sunflower oil cake in batch mode: process stability and kinetic evaluation, Chem. Eng. J. 149 (2009) 70–77, http://dx.doi.org/10.1016/j.cej.2008.10.001.
[30] S. Vieira, R. Hoffmann, Comparison of the logistic and the Gompertz growth functions considering additive and multiplicative error terms, J. R. Stat. Soc. 26 (1977) 143–148, http://dx.doi.org/10.2307/2347021.
[31] A.T. Goshu, P.R. Koya, Derivation of inflection points of nonlinear regression curves: implications to statistics, Am. J. Theor. Appl. Stat. 2 (2013) 268–272, http://dx.doi.org/10.11648/j.ajtas.20130206.25.
[32] C.P. Birch, A new generalized logistic sigmoid growth equation compared with the Richards growth equation, Ann. Bot. 83 (1999) 713–723, http://dx.doi.org/10.1006/anbo.1999.0877.
[33] K.K. Kafle, S.H. Kim, Kinetic study of the anaerobic digestion of swine manure at mesophilic temperature: a lab scale batch operation, J. Biosyst. Eng. 37 (2012) 233–244, http://dx.doi.org/10.5307/JBE.2012.37.4.233.
[34] M.O.L. Yusuf, A. Debora, D.E. Ogheneruona, Ambient temperature kinetic assesment of biogas production form co-digestion of horse and cow dung, Res. Agric. Eng. 57 (2011) 97–104.
[35] M.D. Ghatak, P. Mahanta, Comparison of kinetic models for biogas production rate from saw dust, Carbon 2014 (3) (2014) 248–254, http://dx.doi.org/10.15623/ijret.2014.0307042.